Letters in Applied NanoBioScience
Open-Access Journal (ISSN: 2284-6808)

Article
Volume 14, Issue 1, 2025, 49
https://doi.org/10.33263/LIANBS141.049

Insight into Estrogen Receptor Inhibitory Activity of *Zingiber officinale*-Derived Compounds: *in silico* Studies

Olusola Olalekan Elekofehinti [1,2,*], Folasade Oluwatobiloba Ayodeji [1,2], Ifeoluwa Rachael Adetoyi [2], Foluso Adeola Taiwo [2], Adedotun Olayemi Oluwatuyi [2], Idomeh Festus Aigbokheo [3], Moses Orimoloye Akinjiyan [1,2]

[1] Bioinformatics and Molecular Biology Unit, Department of Biochemistry, Federal University of Technology Akure, Ondo State, P.M.B 704, Akure, Nigeria
[2] Teady Bioscience Laboratory, Akure Ondo State
[3] Blood Sciences (Biochemistry Unit) Pathology First, Synlab, Dobson House, Bentalls, Basildon, Essex, United Kingdom, SS14 3BY
* Correspondence: ooekofehinti@futa.edu.ng, sola_eleko@yahoo.com (O.O.E.);

Scopus Author ID 55316966500
Received: 17.05.2023; Accepted: 11.08.2023; Published: 29.09.2024

Abstract: Breast cancer is one of the most commonly diagnosed forms of the disease, and it is also the leading cause of cancer-related deaths among women worldwide. One of the most important contributors to the development of breast cancer in women is the presence of hormones dependent on estrogen. As a result, there is an urgent need for drugs that are more successful in the fight against this disease. Estrogen receptor (ER) is becoming a target in the therapy of endocrine disorders. The purpose of this research was to identify the most bioactive compounds that can be extracted from *Zingiber officinale*, namely (1R,3S,5R)-1,5-epoxy-3-hydroxy-1-(3,4-dihydroxy-5-methoxyphenyl)-7-(4-dihydroxyphenyl)-heptane, (3S,5S)-3,5-dihydroxy-1-(4-hydroxy-3-methoxyphenyl)-7-(4-hydroxy-3,5-dimethoxyphenyl)-heptane, (R)-linalyl-b-D-glucopyranoside, hexahydrocircumin and 10-gingerol which show promise as ER inhibitors in the search for a breast cancer drug. Schrodinger discovered a wide variety of docking scores during the process of molecular docking. The compounds have drug-like abilities and good ADME properties, and they also displayed satisfactory inhibitory (pIC50 values) ranging from 6.807 to 7.792; as a result, they may be used as effective therapeutic alternatives for the treatment of breast cancer.

Keywords: *Zingiber officinale*; estrogen receptor (ER); cancer; in silico; phytochemicals.

1. Introduction

Breast cancer, the most common type of cancer in women, ranks first as the leading cause of death [1,2]. The incidence of Breast cancer is higher in developing than in developed countries due to late detection [3]. In Nigeria, however, there is an increasing incidence of Breast cancer due to urbanization and lifestyle changes. It is the leading cause of cancer deaths, representing 23% of all cancer cases and 18% of all deaths in Nigeria [4]. Also, there is notably high mortality due to late detection and case presentations. Breast cancer starts in the cells that line the ducts of the glandular tissue of the breast. About 2.3 million new cases of breast cancer were detected in women, leading to 685,000 deaths in 2020 alone. Within the previous five years, a total of 7.8 million living women have been diagnosed with breast cancer [4,5].

Estrogen receptors (ERs) are proteins in cells, and the hormone activates them. The human estrogen receptor has two subtypes: alpha (ER) and beta (ER). They are found in

different tissues where they regulate different sets of genes and have different affinities and activities [6]. Estrogen receptors (ER) are overexpressed in about 74% of breast cancer because cancer cells that are ER-positive depend on estrogen to grow [7]. The presence of high levels of ER in breast epithelium seems to indicate an increased risk of breast cancer. This suggests that ER plays a role in both the beginning and spread of breast cancer [5,8]. Estrogen plays a crucial role in the development of breast cancer; hence, the disruption of the estrogen system via blocking of ER might be a logical approach in the management of breast cancer. To improve survival rates, the majority of current treatments for breast cancer focus on the use of chemotherapy and radiation therapy [9]. The diverse side effects of the current management regimen are of high concern, and the search for alternatives and a complementary approach is still on.

In the last few years, there has been a rise in the use of "natural" or alternative medicines to treat breast cancer due to the lower risk of side effects and the abundance of such substances in nature[10,11]. Ginger rhizome (Zingiber officinale) is a natural plant that is recommended as a cancer treatment to help prevent tumors from growing [12,13]. Because of its taste, color, and spiciness are always added to various foods and drinks. It contains many bioactive compounds that have been shown to have antioxidant, anti-inflammatory, antimicrobial, antiviral, antifungal, antiarthritic, hypotensive, antiatherogenic, radioprotective, and antiemetic properties [14]. Ginger also has compounds like gingerols, gingerdione, shogaols, paradols, caffeic acid, elemene, and zingerone that have been shown to fight cancer. Hence, this study uses a computational approach to investigate the interaction of Zingiber officinale-derived compounds with ER to identify potent compounds that can be deployed to manage breast cancer.

2. Materials and Methods

2.1. Preparation of ligands.

For these in-silico studies, a library of about 53 compounds with low molecular weights was used. The ligands were prepared using the ligprep panel on Maestro 11.5 with an OPLS3 force field at pH 7.0 +/- 2.0 [15]. The options to desalt and generate tautomers were selected, and the stereoisomer computation was set to generate at most 32 per ligand. Maestro was left as the output format.

2.2. Protein preparation.

The ER crystal structure (PDB 1D- 3ERT) was uploaded to Maestro 11.8's workspace. The downloaded protein was prepared using the Schrodinger suite's protein preparation wizard. Bond orders were assigned during protein preprocessing, waters were deleted from 5.0 het groups, and het states were set at pH 7.0 +/- 2.0 [16]. Ions were removed, and a hydrogen bond formed. The H-bond network was optimized using PROPKA in the refine tab; water molecules with fewer than three H-bonds to non-waters were removed [17]. The retrained minimization was performed with an OPLS3 force field and an RMSD of 0.30.

2.3. Receptor grid generation.

A receptor grid generation panel was used to generate the receptor grid file, which represents the active sites of the receptor for glide ligand docking jobs. The ligand-binding site

was defined by selecting the co-crystallized ligand of the protein structure on the workspace. To soften the potential for non-polar parts of the receptor, the van der Waals radii of the receptor atoms with partial atomic charge were scaled by 1.0 and cut by 0.25. The receptor grid box resolution was centered at x, y, and z-axis coordinates 93.91, 68.0, and 9.8.

2.4. Glide extra precision docking.

The prepared compound library was docked into the active site of the protein crystal with extra precision using the flexible ligand sampling set. Model energy score (e-model) was used to select the best-docked structure for each ligand, which combines glide score, non-bonded interaction energy, and excess internal energy of the generated ligand conformation.

2.5. Induced fit docking.

Using the Induced Fit Docking (IFD) allowed for an accurate prediction of the binding affinity of the novel inhibitors to the prepared protein crystal. IFD is an in-silico approach that accurately predicts ligand binding modes and receptor structural changes using Glide and Prime's Refinement module [17,18].

2.6. Calculation of binding free energy.

The Prime MM-GBSA panel was used to calculate the binding free energy for the ligand-receptor complex using Prime's MM-GBSA technology. After energy minimization, MMGBSA quantifies the difference in energy between the free and complex states of both the ligand and the protein. The OPLS3 force field was used in the prime MM-GBA panel, and VSGB was used as the continuum solvent model. Other options were left at their default settings.

The following are the equations for calculating binding energy:

$$\Delta G \text{ bind} = \Delta E + \Delta Gsolv + \Delta GSA \quad (1)$$

$$\Delta E = Ecomplex - E \text{ protein} - Eligand \quad (2)$$

where Ecomplex, Eprotein, and Eligand represent the minimized energies of the protein-inhibitor complex, protein, and inhibitor, respectively.

$$\Delta Gsolv = \Delta Gsolv \text{ (complex)} - \Delta Gsolv \text{ (protein)} - \Delta Gsolv \text{ (ligand)} \quad (3)$$

$$\Delta GSA = \Delta GSA \text{ (complex)} - \Delta GSA \text{ (protein)} - \Delta GSA \text{ (ligand)} \quad (4)$$

where GSA is the surface area's non-polar contribution to solvation energy, the surface energies of complex, protein, and ligand are denoted by GSA (complex), GSA (protein), and GSA (ligand).

2.7. ADMET properties.

The prediction of absorption, distribution, metabolism, excretion, and toxicity (ADMET) is required to establish the safety and drug-ability of the selected compounds [19,20]. The drug-likeness of compounds was determined using Lipinski's rule of five, and this parameter was predicted by Canvas [21–23]. Lipinski's rule of five (RO5) is one of the rules designed to screen compounds, and all selected compounds were evaluated for their respective

drug-like properties using the Swiss ADME online server administered by the Swiss Institute of Bioinformatics [24,25].

2.8. Validation of molecular docking results.

Validation methods are important to ensure a model's robustness on unseen data. The root mean squared error (RMSE) approach is one of the internal validations methods [26–28]. The docking procedure used in this study was affirmed by blasting the FASTA sequence from the ER database server of the CHEMBL. The file was edited in Microsoft Excel to remove entries that did not have a pChEMBL Value. The saved file was then uploaded to Data Warrior to be converted to SDF format (2D structure). The compounds were synthesized and docked with the same protein target used in this study. The screening procedure was deepened using a machine learning-based predictive model (pIC50 Calculation) created by Schrodinger's AutoQSAR panel [29]. Given a learning set of chemical compounds and an activity property from the CHEMBL database, 46 physicochemical and topological descriptors are calculated, along with various Canvas fingerprints [22], yielding an array of independent variables from which to build models. The automated module randomly divided the dataset into 80% training sets and 20% test sets. On each training set, models are created using every feasible combination of machine learning techniques and sets of independent variables supported by each technique [30]. The model's applicability was examined using various statistical parameters such as the correlation coefficient for training sets (R2), the correlation coefficient for test sets (Q2), the root mean square error (RMSE), the standard deviation (SD), and the ranking score [31].

3. Results and Discussion

3.1. Molecular docking analysis.

In this Molecular docking simulation study, 53 ginger derivatives were docked into the ER+ protein receptor (PDB id = 3ERT) binding pocket. Maestro docker software was used because it produces more accurate results than other docking software. The ones with the highest docking scores were selected (the best five), and the remaining compounds are listed in (Table 1). In Table 1, the docking scores and the interactions of all five compounds are shown.

Table 1. The remaining compounds have their docking scores.

S/N	Compounds	Docking Score
1.	(1R,3S,5R)-1,5-epoxy-3-hydroxy-1-(3,4-dihydroxy-5-methoxyphenyl)-7-(4-dihydroxyphenyl)-heptane	-13.204
2	(1R,3S,5R)-1,5-epoxy-3-hydroxy-1-(3,4-dihydroxy-5-methoxyphenyl)-7-(4-hydroxyphenyl)-heptane	-12.339
3	(1R,3R,5R)-1,5-epoxy-3-hydroxy-1-(3,4-dihydroxy-5-methoxyphenyl)-7-(3,4-dihydroxyphenyl)-heptane	-9.911
4	heptan-2-yl-b-D-glucopyranoside	-8.811
5	12-shogaol	-8.692
6	galanal A	-8.582
7	6-isoshogaol	-8.504
8	7-gingerol	-8.428
9	(1R,3S,5R)-1,5-epoxy-3-hydroxy-1-(3,4-hydroxy-5-methoxyphenyl)-7-(4-hydroxy-3-methoxyphenyl)-heptane	-8.401
10	8-shogaol	-8.343
11	4-shogaol	-8.322

S/N	Compounds	Docking Score
12	Curcumin	-8.265
13	(2E, 6E)-3, 7-dimethyl-8-hydroxyoctadien-1-yl-b-D-glucopyranoside	-8.247
14	10-gingerdione	-8.209
15	trans-b-sesquiphellandrol	-8.204
16	galanal B	-8.155
17	neryl-b-D-glucopyranoside	-8.126
18	cis--b-sesquiphellandrol	-8.106
19	(1R,3R,5R)-1,5-epoxy-3-hydroxy-1-(3,4-dihydroxy-5-methoxyphenyl)-7-(4-hydroxy-3-methoxyphenyl)-heptane	-8.042
20	6-shogaol	-7.958
21	(2E, 6Z)-3, 7-dimethyl-8-hydroxyoctadien-1-yl-b-D-glucopyranoside	-7.956
22	6-gingediacetate	-7.938
23	(3S,5S)-3,5-diacetoxy-1,7-bis(4-hydroxy-3-methoxy)-heptane	-7.917
24	4-gingerol	-7.805
25	11	-7.787
26	8-gingerol	-7.772
27	citronellyl-b-D-glucopyranoside	-7.749
28	6-gingerdine	-7.684
29	Aframodial	-7.573
30	6-gingerol	-7.53
31	Curcumin	-7.497
32	geranyl-b-D-glucopyranoside	-7.309
33	6-paradol	-7.282
34	Zingerone	-7.249
35	methyl-6-isogingerol	-6.983
36	5-hydroxy-borneol	-6.891
37	1	-6.891
38	R	-6.857
39	(3S,5S)-6-gingediol4'-O-b-D-glucopyranoside (unfinished)	-6.58
40	1-Dehydro-10-gingerdione	-6.435
41	Zingeberoside A	-6.319
42	6-gingesulfonic acid	-6.279
43	3	-6.26
44	Zingeberoside B(unfinished)	-6.091
45	shogasulfonic acid A	-6.089
46	1,8-epoxy-p-methan-3-yl-b-D-glucopyranoside	-6.088

The first compound had the highest score, which was -13.204kcal/mol. It interacted with the receptor through three normal hydrogen bonds with GLY521, GLU353, and THR347. Hydrophobic interactions are also found with LEU391, MET388, LEU387, LEU428, LEU384, TRP383, MET343, LEU346, LEU349, ALA350, LEU 525, PHE404, VAL418, MET421 and ILE424. It also shows the Predicted (pIC50) value of 7.792. 3D and 2D representations of compound 1 are shown in below Figure 1.

The second compound had a docking score of -9.302kcal/mol, which was the second-best score. It interacted with the receptor through three hydrogen bonds with THR347, ASP351, and VAL534. Hydrophobic interactions are also found with LEU391, MET388, LEU387, LEU384, TRP383, MET343, LEU346, ALA350, LEU354, LEU539, LEU536, PRO535, VAL534, VAL533, CYS530, MET421, ILE424 and LEU525. It also shows the Predicted (pIC50) value of 7.452. 3D and 2D representations of compound 2 are shown in Figure 2.

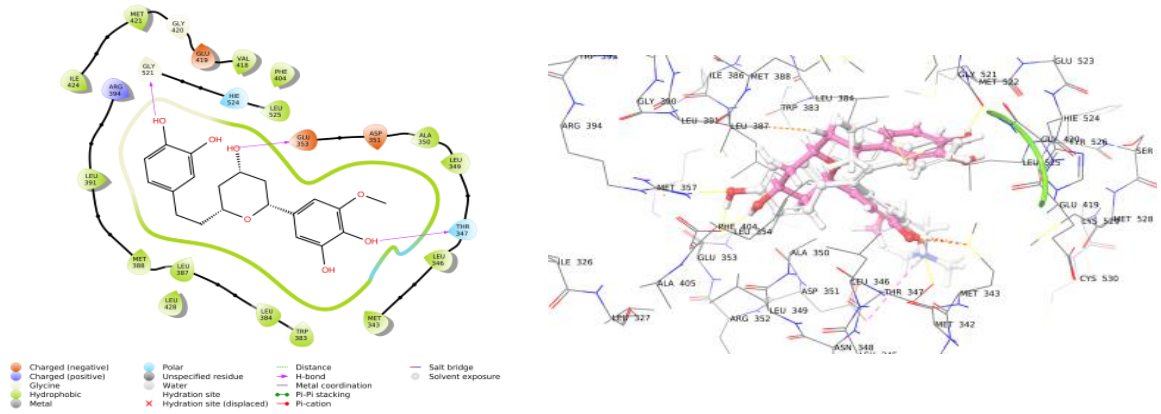

Figure 1. Binding pose of (1R,3S,5R)-1,5-epoxy-3-hydroxy-1-(3,4-dihydroxy-5-methoxyphenyl)-7-(4-dihydroxyphenyl)-heptane with Estrogen Receptor in 2D and 3D structures.

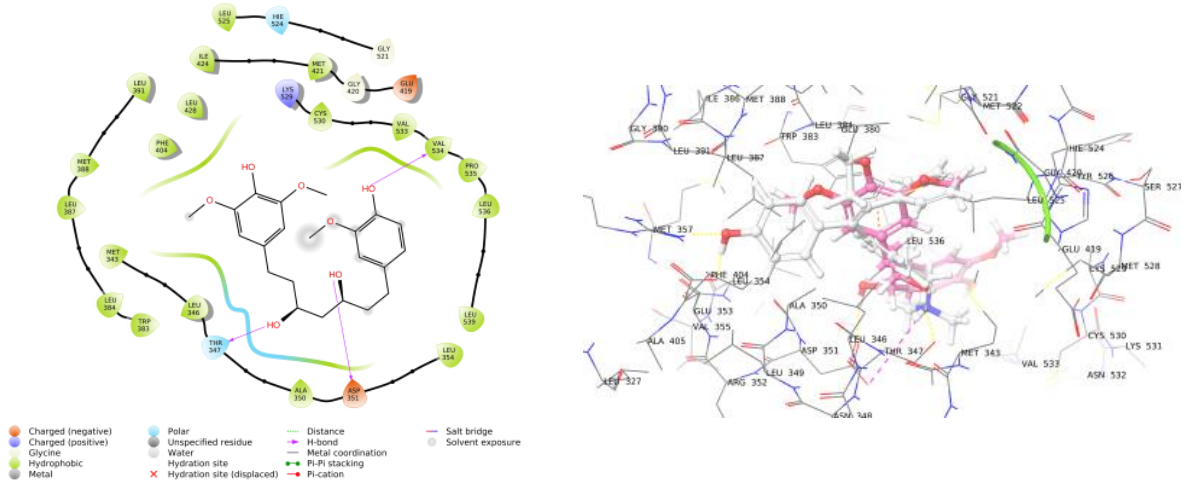

Figure 2. Binding pose of (3S,5S)-3,5-dihydroxy-1-(4-hydroxy-3-methoxyphenyl)-7-(4-hydroxy-3,5-dimethoxyphenyl)-heptane with Estrogen receptor in 2D and 3D structures.

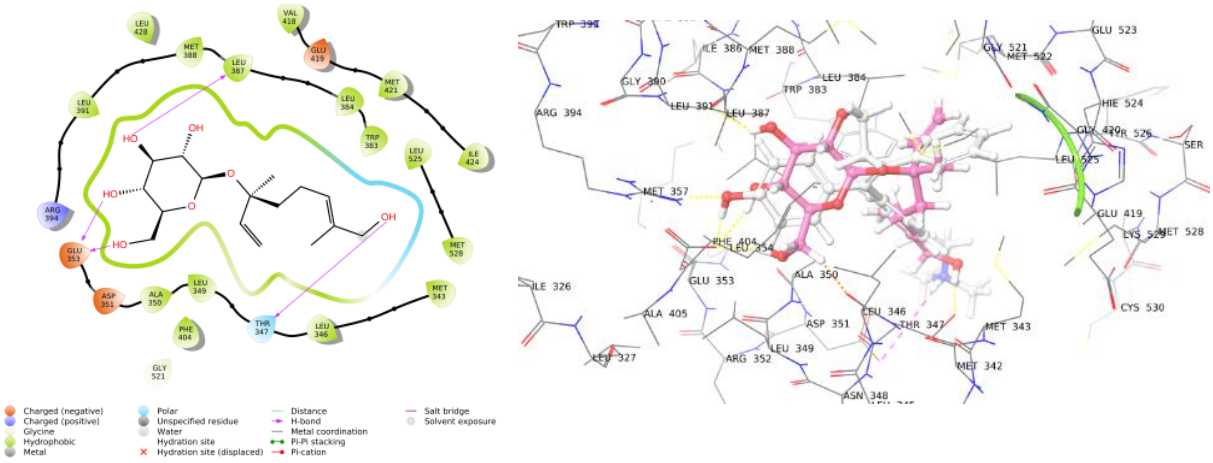

Figure 3. Binding pose of (R)-linalyl-b-D-glucopyranoside with Estrogen Receptor in 2D and 3D structures.

The third compound had -9.162kcal/mol. It was shown that four hydrogen bonds relate to the receptor with GLU353, LEU387, THR347, and GLU353. Hydrophobic interactions are also interacted with ALA350, LEU349, PHE404, LEU346, MET343, MET528, LEU525, TRP383, LEU384, LEU387, MET388, LEU428, LEU 391, ILE424, MET421 and VAL418. It

also shows the Predicted (pIC50) value of 6.807. 3D and 2D representations of compound 3 are shown in Figure 3.

The fourth compound had -9.063kcal/mol. It was shown that four hydrogen bonds relate it to the receptor with LEU387 and ARG394. Hydrophobic interactions are also interacted with LEU391, MET388, LEU387, LEU384, TRP383, MET343, LEU346, LEU349, ALA350, LEU354, LEU525, MET528, LEU536, LEU539 and PHE404 It also shows the Predicted (pIC50) value of 7.452. 3D and 2D representations of compound 4 are shown in Figure 4.

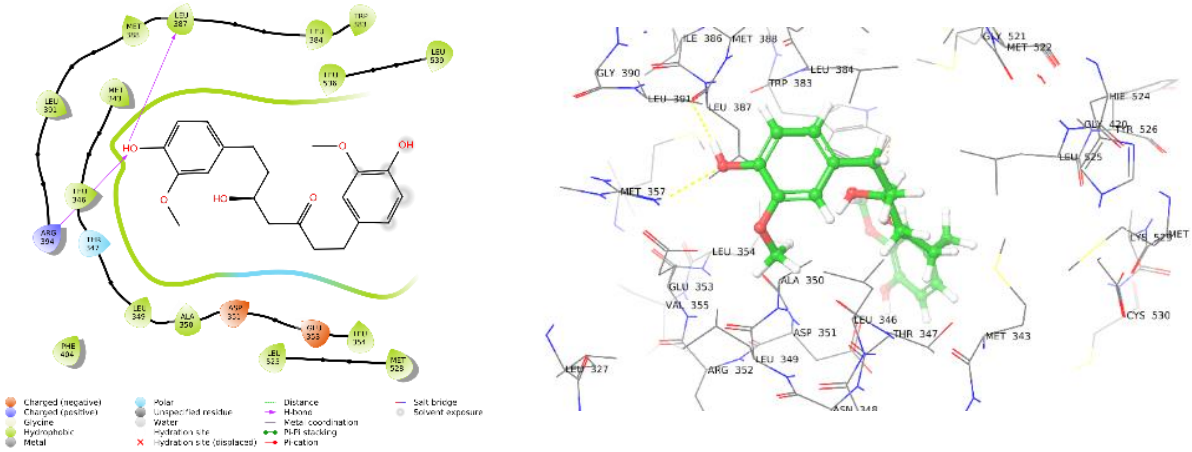

Figure 4. Binding pose of hexahydrocircumin with Estrogen Receptor in 2D and 3D structures.

The fifth compound had -9.03kcal/mol. It was shown that four hydrogen bonds relate to the receptor with ASP351 and GLU353. Hydrophobic interactions are also interacted with TRP383, LEU384, LEU387, MET388, LEU 391, ALA350, LEU349, LEU346, MET343, LEU428, MET421, ILE424, LEU525, MET528 and PHE404. It also shows the Predicted (pIC50) value of 7.217. 3D and 2D representations of compound 5 are shown in Figure 5.

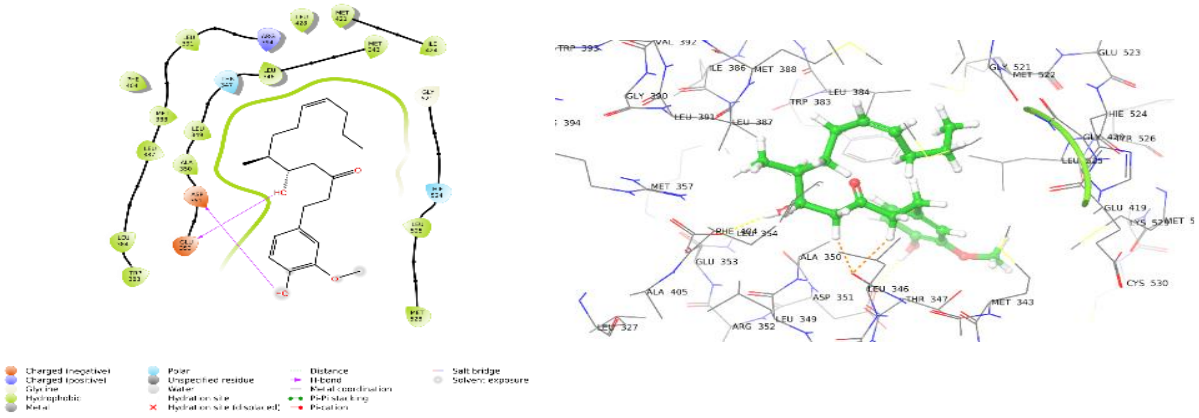

Figure 5. Binding pose of 10-gingerol with Estrogen Receptor in 2D and 3D structures.

3.2. Induced fit docking analysis.

Induced fit docking (IFD) provided a more reliable binding affinity prediction by allowing the protein to rotate upon ligand binding. The hit compounds did not show the same trend when comparing the docking score to the IFD score. (1R,3S,5R)-1,5-epoxy-3-hydroxy-1-(3,4-dihydroxy-5-methoxyphenyl)-7-(4-dihydroxyphenyl)-heptane, which is compound 1 still has the best interaction with the IFD score of – 11.832kcal/mol, 10-gingerol and hexahydrocircumin have a better interaction with each other than the others by measuring IFD

score of – 10.553kcal/ mol and – 9.716kcal/mol respectively. The docking scores and induced fit scores are shown in Table 2.

Table 2. Induced fit docking scores result.

COMPOUNDS NAME	DOCKING SCORE	INDUCED FIT SCORE
(1R,3S,5R)-1,5-epoxy-3-hydroxy-1-(3,4-dihydroxy-5-methoxyphenyl)-7-(4-dihydroxyphenyl)-heptane	-11.832	23.58
(3S,5S)-3,5-dihydroxy-1-(4-hydroxy-3-methoxyphenyl)-7-(4-hydroxy-3,5-dimethoxyphenyl)-heptane	-8.426	27.59
(R)-linalyl-b-D-glucopyranoside	-9.14	29.46
Hexahydrocircumin	-9.716	27.01
10-gingerol	-10.553	24.73

3.3. Binding energy analysis.

The free energy of binding was determined using the MMGBSA post-docking tool, which predicts binding free energies for compounds/ligands by combining molecular mechanics calculations and salvation models. Many studies have shown that the MMGBSA post-docking method is the most reliable for rating the affinity of a ligand on binding to its protein target [32–34] because results obtained through MMGBSA for binding energies calculations were found to be highly reproducible [35,36]. The key energy components to binding free energy were found as ΔGbind, Coulomb interaction (ΔGCoulomb), Hydrogen bond (ΔGHbond), lipophilic energy (ΔGLipo), and ΔGSolv, which boost the binding affinity of the compounds towards the binding pocket of the protein. The evaluation of binding free energy is listed in Table 3.

Table 3. Docking Score with Binding free energy results.

Compounds Name	Docking Score	MMGBSA dG Bind	MMGBSA dG Bind Coulomb	MMGBSA dG Bind Hbond	MMGBSA dG Bind Lipo	MMGBSA dG Bind Solv GB
(1R,3S,5R)-1,5-epoxy-3-hydroxy-1-(3,4-dihydroxy-5-methoxyphenyl)-7-(4-dihydroxyphenyl)-heptane	-13.204	-80.31	-12.21	-1.26	-64.25	25.34
(3S,5S)-3,5-dihydroxy-1-(4-hydroxy-3-methoxyphenyl)-7-(4-hydroxy-3,5-dimethoxyphenyl)-heptane	-9.302	-90.75	-27.47	-1.21	-55.53	34.53
(R)-linalyl-b-D-glucopyranoside	-9.162	-103.3	-23.79	-0.88	-67.72	24.45
hexahydrocircumin	-9.063	-65.34	0.78	-0.59	-48.19	22.95
10-gingerol	-9.03	-102.62	-10.83	-1.35	-76.57	20.91

ΔG bind - MM-GBSA free energy (kcal/mol) of binding; ΔG Bind Coulomb - MM-GBSA free energy of binding (kcal/mol) from the Coulomb energy; ΔG Bind Lipo - MM-GBSA free energy of binding (kcal/mol) from lipophilic binding energy; ΔG Bind Hbond - MM-GBSA free energy of binding (kcal/mol) from hydrogen bonding; ΔG Bind Solv GB – MM-GBSA free energy of binding (kcal/mol) from generalized Born electrostatic solvation energy.

3.4. ADMET analysis.

In Table 4, the reported ADME properties include the number of violations of Lipinski's rule of five (RO5), the molecular weight of the molecule, the predicted octanol–

water partition coefficient, the number of hydrogen bond acceptors, the number of hydrogen bond donors, and the predicted binding to human serum albumin. Lipinski's RO5 is useful for assessing drug-likeness and predicting whether or not small compounds have the potential to be developed into orally active drugs for humans. The rule allows a molecular weight ≤500 Da, octanol–water partition coefficient ≤5, hydrogen bond donor ≤5, and hydrogen bond acceptor ≤10 [37,38]. Prospective drug candidates that obey the RO5 have reduced attrition rates in clinical trials, increasing their chances of becoming and being marketable [39]. *Zingiber officinale* compounds have met this rule. Therefore, they can be used to build ER inhibitors and drugs for breast cancer in the coming years.

Table 4. Result showing ADME properties.

Compounds Name	ROF	MW	AlogP	HBA	HBD	PSA
(1R,3S,5R)-1,5-epoxy-3-hydroxy-1-(3,4-dihydroxy-5-methoxyphenyl)-7-(4-dihydroxyphenyl)-heptane	0	390.432	2.448	7.15	4	109.751
(3S,5S)-3,5-dihydroxy-1-(4-hydroxy-3-methoxyphenyl)-7-(4-hydroxy-3,5-dimethoxyphenyl)-heptane	0	406.475	3.24	7.15	4	107.799
(R)-linalyl-b-D-glucopyranoside	0	332.393	-0.05	10.95	5	121.045
Hexahydrocircumin	0	374.433	3.651	5.7	2	106.947
10-gingerol	0	348.481	4.328	4.2	1	70.165

ROF-Lipinski rule of five; MW-Molecular weight; AlogP- Predictedoctanol/water partition coefficient; HBA-Hydrogen bond acceptor; HBD- Hydrogen bond donor; PSA- Polar surface area.

3.5. AutoQSAR analysis.

In a negative logarithm of inhibitor concentration (pIC50), the observed and predicted activities of the training set and test set were shown on the supplementary list in Table 1.3. The top 5 models are shown in Table 5, and Model kpls_molprint2D_6, the best model, has a standard deviation (S.D.) of 0.5530, R2 of 0.7722, root mean square error (RMSE) of 0.5112 and Q2 of 0.7355. All these values met the necessary criteria for a good QSAR model. The scatter plot in Fig. 6 below compares the experimental and predicted pIC50 values for the best-developed model. Table 1 also shows the predicted pIC50 of the lead compounds using the best model for the data set.

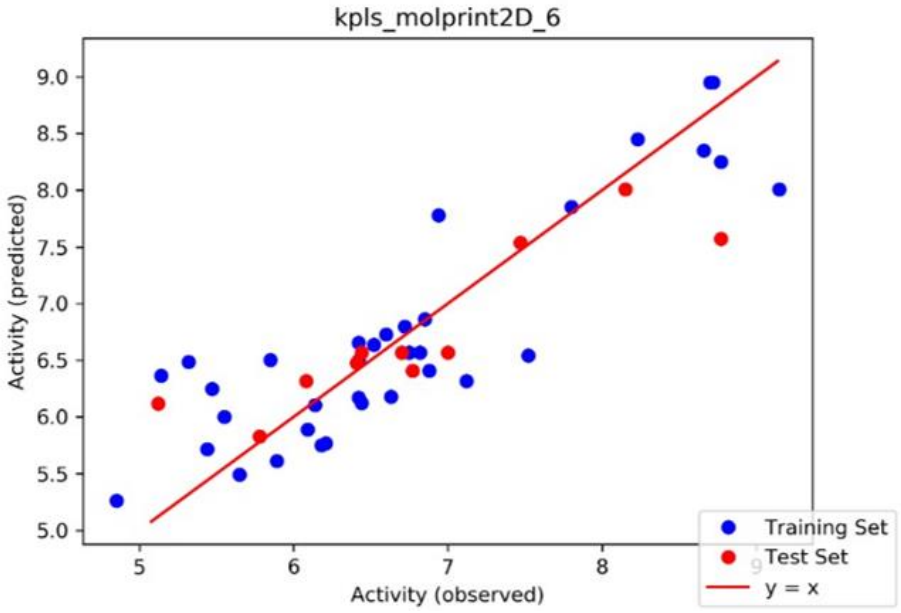

Figure 6. Scatter plot analysis for the best-predicted model from AutoQSAR.

Table 5. Five best models generated by AutoQSAR.

Model code	Score	S.D.	R^2	RMSE	Q^2
kpsl_molprint2D_6	0.7732	0.5530	0.7722	0.5112	0.7355
kpls_molprint2D_39	0.7250	0.5425	0.7764	0.5443	0.7223
mlr_39	0.6547	0.7169	0.6218	0.5332	0.7335
kpls_desc_43	0.6492	0.7092	0.6337	0.6098	0. 6248
pls_49	0.6459	0.6961	0.6451	0.6427	0.6046

4. Conclusions

Estrogen Receptor is a drug target for breast cancer and other diseases. This study demonstrates the ability of compounds derived from *Zingiber officinale* to bind to the Estrogen Receptor, which indicates that these compounds have the potential to act as inhibitors. It is necessary to stress the fact that these compounds have been discovered to have a good docking score, binding free energy, satisfactory ADME properties and inhibitory (pIC50 values) especially (1R,3S,5R)-1,5-epoxy-3-hydroxy-1-(3,4-dihydroxy-5-methoxyphenyl)-7-(4-dihydroxyphenyl)-heptane. Hence, they are potential drugs recommended for the inhibition of ER in breast cancer.

Funding

This research received no external funding.

Acknowledgments

The research acknowledges the technical support received from Teady Bioscience Research Laboratory.

Conflicts of Interest

The authors declare no conflict of interest.

References

1. Su, Z.; Niazi, M.K.K.; Tavolara, T.E.; Niu, S.; Tozbikian, G.H.; Wesolowski, R.; Gurcan, M.N. BCR-Net: A deep learning framework to predict breast cancer recurrence from histopathology images. *PLoS One* **2023**, *18*, e0283562, http://doi.org/10.1371/journal.pone.0283562.
2. Kohler, B.A.; Sherman, R.L.; Howlader, N.; Jemal, A.; Ryerson, A.B.; Henry, K.A.; Boscoe, F.P.; Cronin, K.A.; Lake, A.; Noone, A.-M.; Henley, S.J.; Eheman, C.R.; Anderson, R.N. Annual Report to the Nation on the Status of Cancer, 1975-2011, Featuring Incidence of Breast Cancer Subtypes by Race/Ethnicity, Poverty, and State. *J. Natl. Cancer Inst.* **2015**, *107*, djv048, http://doi.org/10.1093/jnci/djv048.
3. Srinath, A.; van Merode, F.; Rao, S.V.; Pavlova, M. Barriers to cervical cancer and breast cancer screening uptake in low- and middle-income countries: a systematic review. *Health Policy Plan.* **2023**, *38*, 509–527, http://doi.org/10.1093/heapol/czac104.
4. Folorunso, S.A.; Abiodun, O.O.; Abdus-Salam, A.A.; Wuraola, F.O. Evaluation of side effects and compliance to chemotherapy in breast cancer patients at a Nigerian tertiary hospital. *ecancermedicalscience* **2023**, *17*, http://doi.org/10.3332/ecancer.2023.1537.
5. Feng, Y.; Spezia, M.; Huang, S.; Yuan, C.; Zeng, Z.; Zhang, L.; Ji, X.; Liu, W.; Huang, B.; Luo, W.; Liu, B.; Lei, Y.; Du, S.; Vuppalapati, A.; Luu, H.H.; Haydon, R.C.; He, T.-C.; Ren, G. Breast cancer development and progression: Risk factors, cancer stem cells, signaling pathways, genomics, and molecular pathogenesis. *Genes Dis.* **2018**, *5*, 77–106, http://doi.org/10.1016/j.gendis.2018.05.001.
6. Yaşar, P.; Ayaz, G.; User, S.D.; Güpür, G.; Muyan, M. Molecular mechanism of estrogen–estrogen receptor signaling. *Reprod. Med. Biol.* **2017**, *16*, 4–20, http://doi.org/10.1002/rmb2.12006.

7. Brufsky, A.M.; Dickler, M.N. Estrogen Receptor-Positive Breast Cancer: Exploiting Signaling Pathways Implicated in Endocrine Resistance. *Oncologist* **2018**, *23*, 528–539, http://doi.org/10.1634/theoncologist.2017-0423.
8. Zakaria, N.H.; Hashad, D.; Saied, M.H.; Hegazy, N.; Elkayal, A.; Tayae, E. Genetic mutations in HER2-positive breast cancer: possible association with response to trastuzumab therapy. *Hum. Genomics* **2023**, *17*, 43, http://doi.org/10.1186/s40246-023-00493-5.
9. Nik Ab Kadir, M.N.; Mohd Hairon, S.; Ab Hadi, I.S.; Yusof, S.N.; Muhamat, S.M.; Yaacob, N.M. A Comparison between the Online Prognostic Tool PREDICT and MyBeST for Women with Breast Cancer in Malaysia. *Cancers* **2023**, *15*, 2064, http://doi.org/10.3390/cancers15072064.
10. Mitra, S.; Dash, R. Natural Products for the Management and Prevention of Breast Cancer. *Evid. Based Complementary Altern. Med.* **2018**, *2018*, 8324696, http://doi.org/10.1155/2018/8324696.
11. Ali, M.; Wani, S.U.D.; Salahuddin, M.; Manjula, S.N.; K, M.; Dey, T.; Zargar, M.I.; Singh, J. Recent advance of herbal medicines in cancer- a molecular approach. *Heliyon* **2023**, *9*, e13684, http://doi.org/10.1016/j.heliyon.2023.e13684.
12. Prasad, S.; Tyagi, A.K. Ginger and Its Constituents: Role in Prevention and Treatment of Gastrointestinal Cancer. *Gastroenterol. Res. Pract.* **2015**, *2015*, 142979, http://doi.org/10.1155/2015/142979.
13. Rahman, A.; Hannan, A.; Dash, R.; Rahman, H.; Islam, R.; Uddin, J.; Sohag, A.A.M.; Rahman, H.; Rhim, H. Phytochemicals as a Complement to Cancer Chemotherapy: Pharmacological Modulation of the Autophagy-Apoptosis Pathway. *Front. Pharmacol.* **2021**, *12*, 639628, http://doi.org/10.3389/fphar.2021.639628.
14. Mao, Q.-Q.; Xu, X.-Y.; Cao, S.-Y.; Gan, R.-Y.; Corke, H.; Beta, T.; Li, H.-B. Bioactive Compounds and Bioactivities of Ginger (*Zingiber officinale* Roscoe). *Foods* **2019**, *8*, 185, http://doi.org/10.3390/foods8060185.
15. LigPrep, N.Y.N.USA. Release S. *Schrödinger, LLC* **2017**.
16. 4-Epik version 3.8 Release S. . *Schrödinger, LLC, New York, NY, USA.* **2018**.
17. Olsson, M.H.M.; Søndergaard, C.R.; Rostkowski, M.; Jensen, J.H. PROPKA3: Consistent Treatment of Internal and Surface Residues in Empirical pK_a Predictions. *J. Chem. Theory Comput.* **2011**, *7*, 525–537, http://doi.org/10.1021/ct100578z.
18. Sherman, W.; Day, T.; Jacobson, M.P.; Friesner, R.A.; Farid, R. Novel Procedure for Modeling Ligand/Receptor Induced Fit Effects. *J. Med. Chem.* **2006**, *49*, 534–553, http://doi.org/10.1021/jm050540c.
19. Kikiowo, B.; Ogunleye, A.J.; Inyang, O.K.; Adelakun, N.S.; Omotuyi, O.I.; Metibemu, D.S.; David, T.I.; Oludoyi, O.O.; Ijatuyi, T.T. Flavones scaffold of *Chromolaena Odorata* as a potential xanthine oxidase inhibitor: Induced Fit Docking and ADME Studies. *BioImpacts* **2020**, *10*, 227–234, http://doi.org/10.34172/bi.2020.29.
20. Ipinloju, N.; Ibrahim, A.; da Costa, R.A.; Adigun, T.B.; Olubode, S.O.; Abayomi, K.J.; Aiyelabegan, A.O.; Esan, T.O.; Muhammad, S.A.; Oyeneyin, O.E. Quantum evaluation and therapeutic activity of (E)-N-(4-methoxyphenyl)-2-(4-(3-oxo-3-phenylprop-1-en-1-yl) phenoxy)acetamide and its modified derivatives against EGFR and VEGFR-2 in the treatment of triple-negative cancer via in silico approach. *J. Mol. Model.* **2023**, *29*, 159, http://doi.org/10.1007/s00894-023-05543-2.
21. Dayan, G.; Lupien, M.; Auger, A.; Anghel, S.I.; Rocha, W.; Croisetière, S.; Katzenellenbogen, J.A.; Mader, S. Tamoxifen and Raloxifene Differ in Their Functional Interactions with Aspartate 351 of Estrogen Receptor α. *Mol. Pharmacol.* **2006**, *70*, 579–588, http://doi.org/10.1124/mol.105.021931.
22. Duan, J.; Dixon, S.L.; Lowrie, J.F.; Sherman, W. Analysis and comparison of 2D fingerprints: Insights into database screening performance using eight fingerprint methods. *J. Mol. Graph. Model.* **2010**, *29*, 157–170, http://doi.org/10.1016/j.jmgm.2010.05.008.
23. Stępnicki, P.; Wronikowska-Denysiuk, O.; Zięba, A.; Targowska-Duda, K.M.; Bartyzel, A.; Wróbel, M.Z.; Wróbel, T.M.; Szałaj, K.; Chodkowski, A.; Mirecka, K.; Budzyńska, B.; Fornal, E.; Turlo, J.; Castro, M.; Kaczor, A.A. Novel multi-target ligands of dopamine and serotonin receptors for the treatment of schizophrenia based on indazole and piperazine scaffolds–synthesis, biological activity, and structural evaluation. *J. Enzyme Inhib. Med. Chem.* **2023**, *38*, 2209828, http://doi.org/10.1080/14756366.2023.2209828.
24. Yang, H.; Lou, C.; Sun, L.; Li, J.; Cai, Y.; Wang, Z.; Li, W.; Liu, G.; Tang, Y. admetSAR 2.0: web-service for prediction and optimization of chemical ADMET properties. *Bioinformatics* **2019**, *35*, 1067–1069, http://doi.org/10.1093/bioinformatics/bty707.
25. Azad, I.; Khan, T.; Ahmad, N.; Khan, A.R.; Akhter, Y. Updates on drug designing approach through computational strategies: a review. *Future Sci. OA* **2023**, *9*, FSO862, http://doi.org/10.2144/fsoa-2022-0085.

26. Gramatica, P. Principles of QSAR models validation: internal and external. *QSAR Comb. Sci.* **2007**, *26*, 694–701, http://doi.org/10.1002/qsar.200610151.
27. Yasri, A.; Hartsough, D. Toward an Optimal Procedure for Variable Selection and QSAR Model Building. *J. Chem. Inf. Comput. Sci.* **2001**, *41*, 1218–1227, http://doi.org/10.1021/ci010291a.
28. Ojo, O.A.; Ojo, A.B.; Okolie, C.; Nwakama, M.-A.C.; Iyobhebhe, M.; Evbuomwan, I.O.; Nwonuma, C.O.; Maimako, R.F.; Adegboyega, A.E.; Taiwo, O.A.; Alsharif, K.F.; Batiha, G.E.-S. Deciphering the Interactions of Bioactive Compounds in Selected Traditional Medicinal Plants against Alzheimer's Diseases via Pharmacophore Modeling, Auto-QSAR, and Molecular Docking Approaches. *Molecules* **2021**, *26*, 1996, http://doi.org/10.3390/molecules26071996.
29. Sander, T.; Freyss, J.; von Korff, M.; Rufener, C. DataWarrior: An Open-Source Program For Chemistry Aware Data Visualization And Analysis. *J. Chem. Inf. Model.* **2015**, *55*, 460–473, http://doi.org/10.1021/ci500588j.
30. Roy, K.; Das, R.N.; Ambure, P.; Aher, R.B. Be aware of error measures. Further studies on validation of predictive QSAR models. *Chemom. Intell. Lab. Syst.* **2016**, *152*, 18–33, http://doi.org/10.1016/j.chemolab.2016.01.008.
31. Elekofehinti, O.O.; Ejelonu, O.C.; Kamdem, J.P.; Akinlosotu, O.B.; Famuti, A.; Adebowale, D.D.; Iwaloye, O.; Bulu, Y.I.; Kade, I.J.; Rocha, J.B.T. Discovery of potential visfatin activators using *in silico* docking and ADME predictions as therapy for type 2 diabetes. *Beni. Suef Univ. J. Basic Appl. Sci.* **2018**, *7*, 241–249, http://doi.org/10.1016/j.bjbas.2018.02.007.
32. Sun, H.; Li, Y.; Shen, M.; Tian, S.; Xu, L.; Pan, P.; Guan, Y.; Hou, T. Assessing the performance of MM/PBSA and MM/GBSA methods. 5. Improved docking performance using high solute dielectric constant MM/GBSA and MM/PBSA rescoring. *Phys. Chem. Chem. Phys.* **2014**, *16*, 22035–22045, http://doi.org/10.1039/C4CP03179B.
33. Vyshnavi, H.; Namboori, K. Identifying potential ligand molecules EGFR mediated TNBC targeting the kinase domain-identification of customized drugs through in silico methods. *Res. Pharm. Sci.* **2023**, *18*, 121-137, http://doi.org/10.4103/1735-5362.367792.
34. Maffucci, I.; Hu, X.; Fumagalli, V.; Contini, A. An Efficient Implementation of the Nwat-MMGBSA Method to Rescore Docking Results in Medium-Throughput Virtual Screenings. *Front. Chem.* **2018**, *6*, 43, http://doi.org/10.3389/fchem.2018.00043.
35. Duan, H.; Zhang, R.; Yuan, L.; Liu, Y.; Asikaer, A.; Liu, Y.; Shen, Y. Exploring the therapeutic mechanisms of Gleditsiae Spina acting on pancreatic cancer *via* network pharmacology, molecular docking and molecular dynamics simulation. *RSC Adv.* **2023**, *13*, 13971–13984, http://doi.org/10.1039/D3RA01761C.
36. Genheden, S.; Ryde, U. The MM/PBSA and MM/GBSA methods to estimate ligand-binding affinities. *Expert Opin. Drug Discov.* **2015**, *10*, 449–461, http://doi.org/10.1517/17460441.2015.1032936.
37. Rababi, D.; Nag, A. Evaluation of therapeutic potentials of selected phytochemicals against Nipah virus, a multi-dimensional in silico study. *3 Biotech* **2023**, *13*, 174, http://doi.org/10.1007/s13205-023-03595-y.
38. Abdel-Rahman, S.A.; Rehman, A.U.; Gabr, M.T. Discovery of First-in-Class Small Molecule Inhibitors of Lymphocyte Activation Gene 3 (LAG-3). *ACS Med. Chem. Lett.* **2023**, *14*, 629–635, http://doi.org/10.1021/acsmedchemlett.3c00054.
39. Qureshi, F.; Nawaz, M.; Hisaindee, S.; Almofty, S.A.; Ansari, M.A.; Jamal, Q.M.S.; Ullah, N.; Taha, M.; Alshehri, O.; Huwaimel, B.; Break, M.K.B. Microwave assisted synthesis of 2-amino-4-chloro-pyrimidine derivatives: Anticancer and computational study on potential inhibitory action against COVID-19. *Arab. J. Chem.* **2022**, *15*, 104366, http://doi.org/10.1016/j.arabjc.2022.104366.